

## 3 Function

Most functions of the cell, essential for its survival and propagation, are carried out by portents. Several of these functions are biochemical in nature, such as enzymatic activity in breaking down sugars, or transporting oxygen via Hemoglobin. Other functions pertain to sensing the environment, signaling its state, and mounting necessary responses, as in the case of transcription factors interacting with DNA. Still other functions are biophysical, related to force and motion, e.g. transporting organelles, maintaining cell shape, and producing motion. We shall explore examples of the latter in the context of microtubules and motors.

### 3.1 Filaments of the cytoskeleton

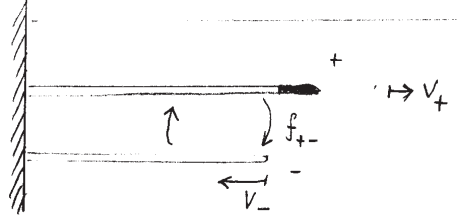
The interior of most cells is far from a fluid bag, but assumes specific shapes and functionalities through the active dynamics of protein fibers forming its *cytoskeleton*. Long fibers are formed by assembling protein units; much like polymers but considerably stiffer due to larger subunits. The thinnest *microfilaments* are made of the monomer *actin* and are roughly 8nm in diameter. *Actin filaments* have a specific directionality (like an arrow), and are typically in a state of dynamic equilibrium in which monomers dissociate from one end (minus side) and assemble at the other end (plus side), in a process called *tread-milling*. In the following, we shall focus on a related dynamic phenomenon in *microtubules*. These are much larger filaments, with diameter of 25nm, assembled from dimers of  $\alpha$  and  $\beta$  *tubulin*. Microtubules are cylinders formed by stacking 13 proto-filaments around a hollow core. They are directional, and of variable length, growing up to 25,000 nm in length. *Intermediate filaments* in the size range of 8 to 25nm occur in a variety of cells, for example strengthening the long axons of neurons.

#### 3.1.1 Dynamic Instability of Microtubules

Discovered in the 1980s, *dynamic instability* is a phenomenon whereby a microtubule grows at a slow, steady rate, then a “catastrophe” is initiated whereby it shortens at a much faster rate, until a “rescue” event restores the original slow growth. This cycle repeats itself (stochastically) on a timescale of several minutes. Key to appreciating the behavior of microtubules, indeed as with the cytoskeleton and the entire cell, is that there is a constant influx of energy. In the case of microtubules, this energy is provided by the hydrolysis of GTP (guanosine tri-phosphate) to GDP (guanosine di-phosphate). The tubulin monomers need to be attached to GTP before they can be added to the growing end of a microtubule. The growing (+) end of the microtubule is thus composed of GTP bound tubulin. Further behind this cap, some GTP molecules can hydrolyze to GDP, releasing around  $10k_B T$  of energy in the process. The resulting GDP rich region is less stable, and GDP bound tubulin can detach from the other (-) end. We shall first address how the addition and detachment of tubulins can lead to a dynamic steady state, and then inquire if the rapid dynamic changes are due to instabilities in the cap.

### 3.1.2 Microtubule Growth and Regulation

To study the dynamic behavior of a microtubule (MT), we examine a simple two state model:<sup>1</sup> The MT is either slowly growing with velocity  $v_+$ , or rapidly shrinking with velocity  $v_-$ . Assuming that one end of the MT is attached to a stationary support at  $z = 0$ , the growing (+) end can be at a distance  $z$  at time  $t$ . With probability  $p_+(z, t)$  the MT is growing, while with probability  $p_-(z, t)$  it has lost its GTP cap and is shrinking. There is a probability that a catastrophe occurs, switching from a growing to a shrinking MT, at a rate  $f_{+-}$ , while the converse rescue events occur at rate  $f_{-+}$ .



The two probability functions evolve according to the coupled equations

$$\begin{aligned}\frac{\partial p_+(z, t)}{\partial t} &= -f_{+-}p_+(z, t) + f_{-+}p_-(z, t) - \frac{\partial}{\partial z}(v_+p_+) , \\ \frac{\partial p_-(z, t)}{\partial t} &= +f_{+-}p_+(z, t) - f_{-+}p_-(z, t) + \frac{\partial}{\partial z}(v_-p_-) .\end{aligned}\quad (3.1)$$

For simplicity, we have assumed a continuously variable length  $z$ ; a more microscopic representation would describe the evolution of  $p_{\pm}(n, t)$  for  $n$  tubulin units, with rates for addition/subtraction of units. The above coupled partial differential equations are linear, and hence easily solved by Fourier transforming in space and time, as

$$p_{\pm}(z, t) = \int dk d\omega e^{ikz - i\omega t} \tilde{p}_{\pm}(k, \omega). \quad (3.2)$$

Effectively this amounts to the replacements

$$\frac{\partial}{\partial t} \rightarrow -i\omega, \quad \frac{\partial}{\partial z} \rightarrow ik, \quad (3.3)$$

which after simple manipulations lead to the matrix equation

$$\begin{pmatrix} i\omega - f_{+-} - ikv_+ & f_{-+} \\ f_{+-} & i\omega - f_{-+} + ikv_- \end{pmatrix} \begin{pmatrix} \tilde{p}_+(k, \omega) \\ \tilde{p}_-(k, \omega) \end{pmatrix} = 0. \quad (3.4)$$

For the matrix equation to have non-zero solutions, the determinant of the  $2 \times 2$  matrix must be zero. This condition leads to a dispersion equation that relates  $\omega$  to  $k$  as

$$\omega(k) = vk - Dk^2 + \dots . \quad (3.5)$$

---

<sup>1</sup>M. Dogterom and S. Leibler, *Phys. Rev. Lett.* **70**, 1347 (1993).

The term linear in  $k$  represents the net drift velocity, while the quadratic term describes an effective diffusion due to the switchings between the two states. The details of this calculation are left to the problem set. We shall instead derive expressions for  $v$  and  $D$  by appealing to physical arguments.

Consider the limit where exchanges between  $+$  and  $-$  states take place rapidly. This quickly leads to an equilibrium between the two states such that

$$\frac{p_+}{p_-} \approx \frac{f_{-+}}{f_{+-}}, \quad \implies \quad p_+ = \frac{f_{-+}}{f_{+-} + f_{-+}}, \quad \text{and} \quad p_- = \frac{f_{+-}}{f_{+-} + f_{-+}}. \quad (3.6)$$

The evolution of the net probability  $p(z, t) = p_+(z, t) + p_-(z, t)$  for MTs of length  $z$  is then obtained by adding the two evolution Eqs. (3.1), as

$$\frac{\partial p(z, t)}{\partial t} = -\frac{\partial}{\partial z} (v_+ p_+ - v_- p_-), \quad (3.7)$$

which using Eq. (3.6) turns into

$$\frac{\partial p(z, t)}{\partial t} = -\frac{\partial}{\partial z} \left[ \left( v_+ \frac{f_{-+}}{f_{-+} + f_{+-}} - v_- \frac{f_{+-}}{f_{-+} + f_{+-}} \right) p \right]. \quad (3.8)$$

The solution to the above equation is a traveling wave  $p(z, t) = p(z - vt)$  describing a net probability that drifts along the  $z$  axis with a velocity

$$v = \frac{f_{-+} v_+ - f_{+-} v_-}{f_{-+} + f_{+-}}. \quad (3.9)$$

Of course, given the barrier at  $z = 0$ , the above solution only makes sense as long as  $v$  is positive. When the value of  $v$  from Eq. (3.9) is negative, the MTs tend to shrink towards zero. In this case fluctuations lead to a time independent steady state in which

$$p_{\pm}(z, t) = p_{\pm}^*(z) = c_{\pm} e^{-\alpha z}. \quad (3.10)$$

This can be verified by substituting Eq. (3.10) into Eqs. (3.1) to obtain the matrix form

$$\begin{pmatrix} -f_{+-} + \alpha v_+ & +f_{-+} \\ +f_{+-} & -f_{-+} - \alpha v_- \end{pmatrix} \begin{pmatrix} c_+ \\ c_- \end{pmatrix} = 0. \quad (3.11)$$

Once again, the determinant of the matrix must be zero to allow non-zero solutions, leading to

$$\alpha = \frac{f_{+-} v_- - f_{-+} v_+}{v_- v_+}. \quad (3.12)$$

The probability to find a MT of length  $z$  in this state is a simple exponential with

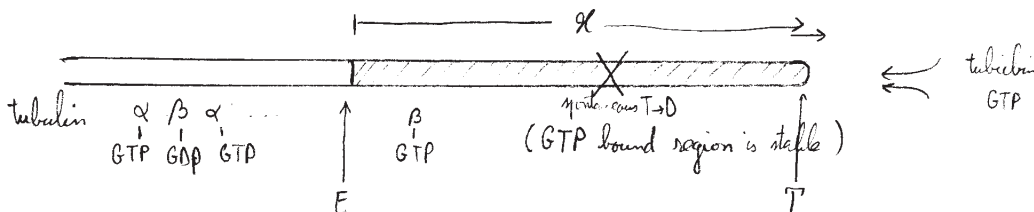
$$\langle z \rangle = \frac{1}{\alpha} = \frac{v_- v_+}{f_{+-} v_- - f_{-+} v_+}, \quad (3.13)$$

while the fraction of time the MT is in the growing/shrinking state is easily observed to be

$$\frac{c_+}{c_-} = \frac{v_-}{v_+}. \quad (3.14)$$

### 3.1.3 Caps & Catastrophes

In the last section we treated the transitions between the growing and shrinking states as instantaneous, effectively examining the MTs at time and length scales much longer than those of individual molecules. We would like to now take a closer look at the events that initiate the catastrophes. As noted earlier, the  $\alpha$  and  $\beta$  tubulin molecules that attach to the + end are bound to GTP. The presence of the GTP at, and near, the growing tip stabilizes the MT. Further away from the tip, the GTP attached to  $\beta$ -tubulin (but not that attached to  $\alpha$ -tubulin) can hydrolyze to GDP, releasing some energy. This renders the MT susceptible to breakdown and shrinkage. The cap region prevents this breakdown, maintaining the GDP bound portion in a metastable state. However, if through stochastic fluctuations the cap region disappears, the protofilaments start to fray and the MT rapidly shrinks until another cap is formed (a rescue event).



Let us focus on the cap region of the MT, assumed to span a length  $x$  from the tip  $T$  at the + end to a location  $E$  which marks the start of the GDP rich portion of the MT. The length  $x$  can change due to the following processes:

- The tip  $T$  grows at a rate  $g(c)$  that depends on the concentration of tubulin.
- The end  $E$  moves at a rate  $h$  related to how fast the hydrolyzed front advances along the MT. This rate is presumably independent of the tubulin concentration.

If this is all, the cap region should grow/shrink with an average velocity of  $v = g(c) - h$ . However, there will certainly be stochastic fluctuations, which by analogy to the example considered earlier should be described by the equation

$$\partial_t p(x, t) = -\partial_x(vp) + D\partial_x^2 p, \quad (3.15)$$

for the probability  $p(x, t)$  of a cap of length  $x$ , where  $D$  is some effective diffusion coefficient. However, for  $v > 0$  the above equation predicts a cap that grows indefinitely and the probability of catastrophe becomes negligible, while for  $v < 0$  a catastrophe should occur at a short time set by the initial cap length. These predictions of the model are at variance with experimental observations. For example, the model would predict longer cap lengths in solutions rich in tubulin (along with faster MT growth). If such rapidly growing MTs are then transferred to a solution poor in tubulin (such that  $v$  becomes negative), the prediction is that the onset of catastrophes should be later for MTs transferred from solutions rich in

tubulin (longer initial caps). This contradicts the observation that the onset of catastrophes is independent of the quality of the initial solution.

One potential solution is to note that hydrolysis events may occur not just at the boundary point E, but throughout the cap.<sup>2</sup> Introducing hydrolyzed GDP at some point  $y$  along the cap, effectively fragments it, creating a shorter cap of length  $y$  (with the portion from  $y$  to  $x$  falling away). Since such events can occur at any point along the cap, they should be described by a *rate per unit length*, which we denote by  $r$ . The introduction of  $r$  modifies Eq. (3.15) to

$$\partial_t p(x, t) = -\partial_x(vp) + D\partial_x^2 p - rxp + r \int_x^\infty dyp(y, t). \quad (3.16)$$

The negative term takes into account the reduction in probability of MTs of length  $x$  due to hydrolysis at a rate proportional to  $x$ ; the positive term adds the probabilities for appearance of a segment of length  $x$  due to fragmentation of longer segments.

Equation (3.16) is an integral–differential equation, but in terms of the cumulative probability

$$\int_x^\infty dyp(y, t) \equiv \bar{P}(x, t) = 1 - P(x, t), \quad (3.17)$$

is equivalent to

$$\partial_t \bar{P}(x, t) = -\partial_x(v\bar{P}) + D\partial_x^2 \bar{P} - rx\bar{P}, \quad (3.18)$$

as can be verified by applying  $-\partial_x$  to both sides. Equation (3.18) no longer has the integral character, and is thus easier to solve. Rather than a formal solution, we shall determine the key features of the behavior pertaining to catastrophes:

- In good solutions (rich in tubulin)  $v > 0$ , and the natural tendency of the cap is to grow longer. This is opposed mostly by the fragmentation events (and to a smaller extent by stochastic diffusion which we shall ignore initially). After a transient period, the competition between growth and fragmentation leads to a steady state distribution  $p^*(x)$  for cap sizes. Setting  $D = 0$ , this stationary solution is easily obtained from Eq. (3.18) as

$$\log \bar{P}^*(x) = -\frac{rx^2}{2v}, \quad \Rightarrow \quad \bar{P}^*(x) = e^{-\frac{rx^2}{2v}}, \quad \Rightarrow \quad p^*(x) = -\frac{d\bar{P}^*(x)}{dx} = \frac{rx}{v} e^{-\frac{rx^2}{2v}}. \quad (3.19)$$

(Note the boundary conditions  $\bar{P}^*(0) = 1$  and  $\bar{P}^*(\infty) = 0$ .) Because of fragmentation the cap does not grow indefinitely, but stabilizes to a typical size

$$\langle x \rangle = \sqrt{\frac{\pi v}{2r}}, \quad (3.20)$$

which becomes longer as the tubulin concentration and  $v$  increases. For  $v > 0$ , there can be no catastrophes if diffusion is ignored. This is because while fragmentation can create short caps, the new cap starts growing away from  $x = 0$ . We thus reintroduce  $D$  as a small perturbation acting on this steady state, and note that Eq. (3.18) now gives

$$\partial_t \bar{P}(0, t) = -\frac{Dr}{v} \bar{P}(0, t), \quad \Rightarrow \quad \bar{P}(0, t) = e^{-\frac{Dr}{v}t}, \quad (3.21)$$

---

<sup>2</sup>H. Flyvbjerg, T.E. Holy, and S. Leibler, Phys. Rev. Lett. **73**, 2372 (1994).

indicating a simple exponential decay. Catastrophes are thus Poisson distributed occurring at a rate  $Dr/v$ .

- The situation is very different in tubulin poor solutions with  $v < 0$ . In this case, fragmented caps shrink to zero length, initiating catastrophes. Starting with a long cap, a catastrophe occurs at time  $t$  if a hydrolysis event takes place at some time  $0 < \tau < t$  at a position  $x(\tau) = (t - \tau)|v|$  so that the fragment can shrink to zero in  $(t - \tau)$ . The probability  $p_{\text{cat}}(t)dt$  of a catastrophe in the interval  $[t, t + dt]$  is thus the product of the probabilities that there are no hydrolysis events in the domain  $0 < x < x(\tau)$  for  $0 < \tau < t$ , and that there is a hydrolysis event at the border of this region. Since the area of the domain is  $|v|t^2/2$ , and the hydrolysis events are Poisson distributed, we find

$$p_{\text{cat}}(t) = r|v|te^{-r|v|t^2/2}. \quad (3.22)$$

The mean time between catastrophes is thus

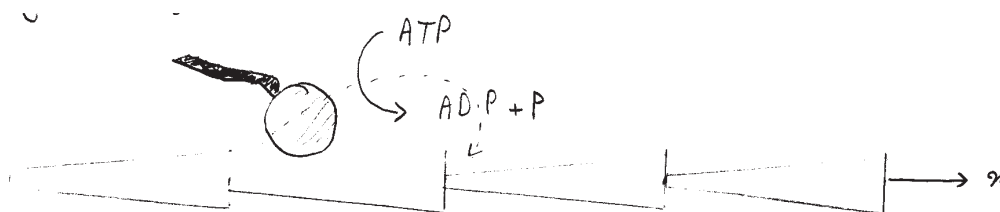
$$\langle t \rangle_{\text{cat}} = \sqrt{\frac{\pi}{2r|v|}}. \quad (3.23)$$

This result is quite insensitive the initial length of the cap, explaining experiments in which MTs are transported from good to poor solutions.

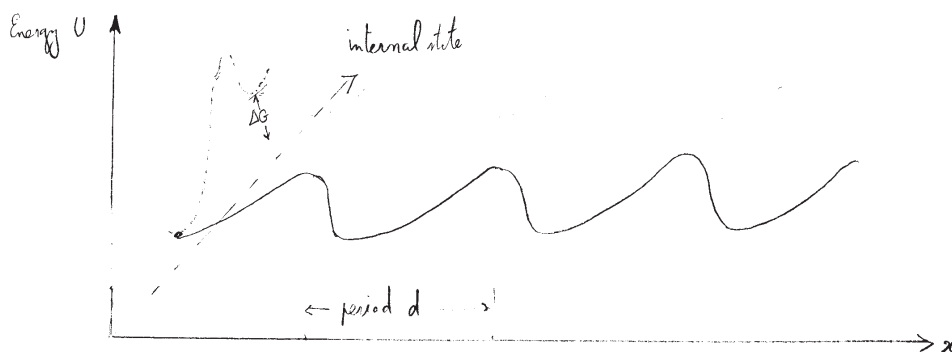
## 3.2 Molecular Motors

A variety of cellular processes requiring mechanical work, such as movement, transport and packaging material, are performed with the aid of *protein motors*. These molecules consume fuel, typically from conversion of ATP to ADP, to generate force and motion. Unlike macroscopic engines which proceed deterministically through a cycle, the tiny molecular machines are constantly agitated by thermal fluctuations and their operation is inherently stochastic. There are two common elements to most molecular motors:

- An *asymmetry* that determines the direction of motion. In the case of *myosin* this is provided by the polarity of actin filaments along which it moves, e.g. in contracting muscles. *Kinesin* and *dynein* are two motors that transport cargo along microtubules (MTs), but in opposite directions; kinesin moving to the (+) end, and dynein towards the (-) end.



- The asymmetry encountered by motors is reminiscent of ratchets: The motor experiences a periodic but asymmetric potential along its track. However, it is well known that *Brownian ratchets* cannot extract energy from thermal fluctuations. In equilibrium there is no directed motion despite asymmetry, and an energy consuming mechanism is needed to rectify motion in a ratchet potential. A general scheme is for the motor to have a number of internal

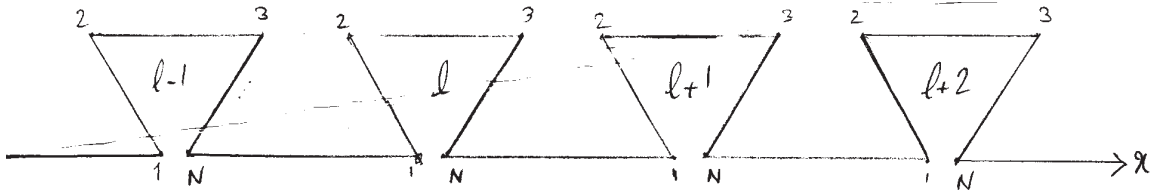


states, e.g. bound to ATP or ADP, each of which experiences a different ratchet potential. As we shall see, moving between the internal states enables trapping and rectifying the fluctuations. We can get a rough estimate of the forces generated by molecular motors as follows: A typical step size for kinesin along a MT is  $a \approx 8.2\text{nm}$ , and the energy released by hydrolysis of one ATP molecule in physiological conditions is about  $\Delta G_h = 12k_B T$ . Assuming

the energy released by hydrolysis of a single ATP is completely used up leads to a maximal possible force of  $F_{\max} = \Delta G_h/a \approx 6.2$  pN.

### 3.2.1 Asymmetric Hopping

Rather than working with a continuous ratchet potential, we can capture much of the same physics by examining so called asymmetric hopping models,<sup>3</sup> in which the motor makes discrete jumps along its track. However, at each site along the track, it can be in a discrete number of internal states. For example, in the system depicted below, there are 4 internal states at each site, e.g. corresponding to: MT, MT+ATP, MT+ADP+P, MT+ADP. One then assigns rates for transitions along the track and between internal states. With proper choice of asymmetric rates the motion can be biased in one direction.



Let us demonstrate the procedure and the constraints involved for a simple model with only two internal states, say representing the motor bound to ATP or ADP. We shall denote the rates for transitions between the two internal states by  $u$  and  $d$ . As the motor moves to the next site along the track it must change its internal state, and we assign asymmetric rates of  $r$  and  $l$  for moving to the right ( $T \rightarrow D$ ) and the left ( $D \rightarrow T$ ) respectively. The Master equations governing the evolution of probabilities for these states are

$$\begin{aligned} \frac{dp_D(n, t)}{dt} &= lp_T(n+1) + dp_T(n) - (u+r)p_D(n) \\ \frac{dp_T(n, t)}{dt} &= rp_D(n-1) + up_D(n) - (d+l)p_T(n). \end{aligned} \quad (3.24)$$

For slowly varying probabilities, the continuum form of these equations is

$$\begin{aligned} \frac{\partial p_D(x, t)}{\partial t} &= (l+d)p_T(x) - (u+r)p_D(x) + al \frac{\partial}{\partial x} p_T(x, t) + \frac{a^2 l}{2} \frac{\partial^2}{\partial x^2} p_T(x, t) \\ \frac{\partial p_T(x, t)}{\partial t} &= (r+u)p_D(x) - (d+l)p_T(x) - ar \frac{\partial}{\partial x} p_D(x, t) + \frac{a^2 r}{2} \frac{\partial^2}{\partial x^2} p_D(x, t). \end{aligned} \quad (3.25)$$

We can extract the behavior of the above equations for slow and long wavelength variations by first noting that (relatively) rapid interconversion between internal states leads to a local equilibrium in which

$$(l+d)p_T(x) = (u+r)p_D(x), \quad (3.26)$$

<sup>3</sup>M.E. Fisher and A.B. Kolomeisky, PNAS **96**, 6597 (1999).

or in terms of the net probability,  $p(x) = p_T(x) + p_D(x)$ ,

$$p_T(x) = \frac{u+r}{u+d+r+l} p(x) \quad \text{and} \quad p_D(x) = \frac{d+l}{u+d+r+l} p(x). \quad (3.27)$$

Adding the two Eqs (3.25) and substituting from Eq. (3.27) leads to a standard drift-diffusion equation for  $p(x, t)$ , with drift velocity

$$v = a \frac{rd - lu}{u+d+r+l}, \quad (3.28)$$

and diffusion coefficient

$$D = \frac{a^2}{2} \frac{rd + lu + 2lr}{u+d+r+l}. \quad (3.29)$$

The requirement of thermal equilibrium places stringent constraints on any pair of forward/backward reaction rates. In the absence of external force, and in thermal equilibrium, the transition rates are related to the energies of the different states by

$$\frac{u}{d} = \frac{r}{l} = \exp[-\beta(U_{M+T} - U_{M+D})] = e^{-\beta\Delta U_M}, \quad (3.30)$$

and in this case there is no net velocity,  $v = 0$ . The hydrolysis of ATP provides a (non-equilibrium) source of energy, such that

$$\frac{r}{l} = \frac{u}{d} \cdot e^{\beta\Delta G_h}. \quad (3.31)$$

Substituting these forms in the equation for drift velocity, we find

$$v = a \frac{lu}{u+d+r+l} \left( \frac{r}{l} \frac{d}{u} - 1 \right) = \frac{alu}{u+d+r+l} (e^{\beta\Delta G_h} - 1) > 0. \quad (3.32)$$

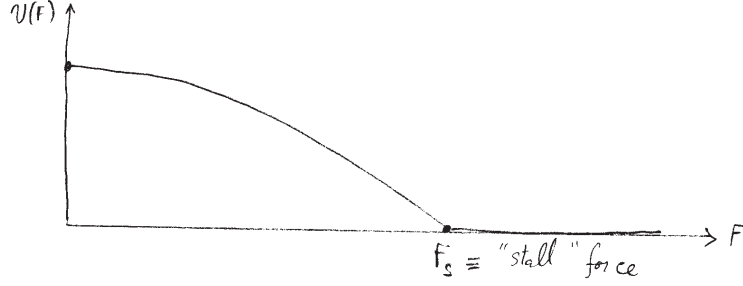
### 3.2.2 Force of a Brownian Motor

To find out how efficiently the energy input from ATP is converted to work, we need to know the force exerted by the motor in traveling a distance  $a$  at each step. This is not an easy task as it is not possible to directly measure all dissipative and other forces acting on the small molecule. The following procedures have been used to estimate forces on the motor.

**The stall force** is obtained by pulling the motor back with an optical tweezer. The motor must now also climb up against the potential from the external force  $F$ , resulting in

$$\frac{r}{l} \Big|_F = \frac{r}{l} \Big|_0 e^{-\beta Fa} \quad \text{and} \quad v = a \frac{lu}{u+d+r+l} (e^{\beta(\Delta G_h - Fa)} - 1). \quad (3.33)$$

Clearly the motor stalls ( $v = 0$ ) when  $F = F_s = F_{\max} = \Delta G_h/a$ . This agrees with our previous rough estimate, as there are no frictional forces (and corresponding dissipate losses) for a stationary motor.



**The Einstein force** is obtained by analogy to Brownian particles from a ratio of velocity and diffusion coefficients. A particle in solution experiences a drag force proportional to its velocity, such that  $v = \mu F$  where  $\mu$  is its *mobility*. In the absence of an external force, the particle diffuses in solution with diffusion constant  $D$ . Diffusion originates in collisions with thermally excited atoms in the fluid, and to ensure proper thermal equilibrium the mobility and diffusion constant must be related by the *Einstein relation*,  $D = \mu k_B T$ . From these relations we can define an Einstein force

$$F_E = k_B T \frac{v}{D} = \frac{2k_B T}{a} \frac{rd - lu}{rd + lu + 2lr} = \frac{2k_B T}{a} \frac{\frac{rd}{lu} - 1}{\frac{rd}{lu} + 1 + 2\frac{r}{u}}, \quad (3.34)$$

where we have used the values for drift and diffusion of the motor along its track from the two-state hopping model. Since  $(rd)/(lu) = e^{\beta \Delta G_h}$ , in the limit  $\beta \Delta G_h \rightarrow 0$

$$F_E \approx \frac{F_{\max}}{1 + r/u},$$

while for  $\beta \Delta G_h \gg 1$ ,  $F_E \approx 2k_B T/a$ . Thus the Einstein force is always less than the maximum possible force, and limited by thermal fluctuations.

### 3.3 Brownian Motion

For simplicity, we focus on one coördinate  $x$  and how it changes with  $t$ . According to Mr. Newton, the acceleration is due to the applied forces. When the particle at  $x$  is immersed in fluid, we find the effective force includes both a potential term and an inverse-mobility term due to viscosity:

$$m\ddot{x} = -\frac{\partial V}{\partial x} - \frac{1}{\mu}\dot{x}. \quad (3.35)$$

For a sphere of radius  $a$ , the Stokes relation gives the viscous drag mobility as

$$\mu = \frac{1}{6\pi a\eta}, \quad (3.36)$$

where  $\eta$  is the fluid's viscosity. In the regime of low Reynolds number, we can neglect the left-hand side of Eq. (3.35), giving

$$\dot{x} = -\mu\frac{\partial V}{\partial x}.$$

If this were the whole story, the motion would be rather boring. However, empirical observations lead us to include an extra term, for the stochastic effects of fluid molecules impacting the big particle on all sides:

$$\dot{x} = -\mu\frac{\partial V}{\partial x} + \eta(t). \quad (3.37)$$

Two notable properties of the noise function  $\eta(t)$  are the following:

$$\langle \eta(t) \rangle = 0, \quad (3.38)$$

$$\langle \eta(t)\eta(t') \rangle = 2D\delta(t-t'). \quad (3.39)$$

$$p[\eta(t)] \propto \exp\left[-\frac{1}{2D}\int^t \eta(t')^2 dt'\right]. \quad (3.40)$$

For  $V = 0$ ,  $\dot{x} = \eta(t)$ , and

$$x(t) = \int^t dt' \eta(t').$$

The mean dispersion is zero:

$$\langle x(t) \rangle = 0, \quad (3.41)$$

while the mean-squared dispersion is given by

$$\langle x^2(t) \rangle = \int^t dt'_1 dt'_2 \langle \eta(t'_1)\eta(t'_2) \rangle = 2Dt. \quad (3.42)$$

If  $V$  is position-dependent, it is best to think of the probability  $p(x, t)$  to find our particle at position  $x$  at some time  $t$ . By various steps of algebra, we can convert Eq. (3.37) into

$$\frac{\partial p(x, t)}{\partial t} = -\frac{\partial J}{\partial x}, \quad (3.43)$$

where  $J$  is the *probability current*.  $J$  has two components:

$$J = v(x)p(x, t) - D \frac{\partial p}{\partial x}, \quad (3.44)$$

where  $v(x)$  is defined as  $\mu \partial_x V$ . The ultimate answer is that the probability satisfies the following equation:

$$\boxed{\partial_t p(x, t) = -\partial_x(v(x)p) - D \partial_x^2 p}, \quad (3.45)$$

which is our old friend, the Fokker-Planck equation. The steady-state solution to which, we recall, is

$$p^*(x) \propto \exp\left(-\frac{\mu}{D}V(x)\right). \quad (3.46)$$

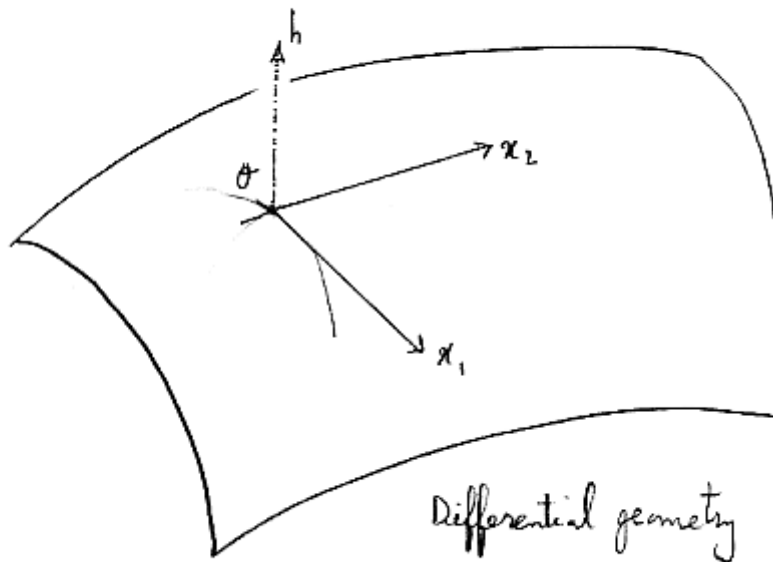
According to Boltzmann, the probability  $p^*(x)$  must be proportional to  $e^{-\beta V(x)}$ , implying that the diffusion constant  $D$  is given by

$$\boxed{D = \mu k_B T}. \quad (3.47)$$

Eq. (3.47) is known as the *Einstein relation*.

### 3.4 Cell Membranes

The first topic we need to address is how we describe a curved membrane. Once we have an energy function (or functional), we can use it to address several intriguing topics, including the reason red blood cells have their characteristic double-dimpled shape.



Imagine that we have a two-dimensional film, like a soap bubble stretched across a frame. We blow gently over the bubble and watch it wiggle. With what tools can we describe the shape of this film? This takes us into the regime of *differential geometry*. We can characterize the film's shape in the following way:

Pick a point  $O$  on the film, and draw the plane tangent to the surface at  $O$ . Choose a pair of coordinates  $(x_1, x_2)$  on the tangent plane. In the close vicinity of  $O$ , the tangent plane and the surface coincide. How do the surface and the tangent plane separate as we move away from  $O$ ? (You can tell that this is a physicist talking here.) We measure the "height"  $h(x_1, x_2)$  between the tangent plane and the surface along the normal vector at point  $O$ .

When we expand  $h(x_1, x_2)$ , the first terms that can appear are quadratic:

$$h(x_1, x_2) = \frac{1}{2} \sum_{i,j=1}^2 c_{ij} x_i x_j + \mathcal{O}(x^3). \quad (3.48)$$

Here, the matrix  $c_{ij}$  is given by

$$c_{ij} = \left. \frac{\partial^2 h}{\partial x_i \partial x_j} \right|_{x=0}, \quad (3.49)$$

which is a  $2 \times 2$  *curvature tensor*. It is not the most ideal description of the curvature, because it depends upon our choice of coördinate axes. We need to look for properties of  $c_{ij}$  which are invariant under changes of coördinates. One such property is the trace, or sum over the diagonal elements. We can tell this is true because we could diagonalize the matrix, making the diagonal elements the eigenvalues—which do not change under rotations. Symbolically,

$$\text{Tr } C = c_{11} + c_{22} = \frac{1}{R_1} + \frac{1}{R_2} \equiv 2H. \quad (3.50)$$

We have written the eigenvalues as  $1/R_i$  for dimensional reasons, since they have the units of inverse length. The trace, sometimes denoted  $H$ , is known as the *mean curvature*.

Another invariant properties is the determinant,

$$\det C = c_{11}c_{22} - c_{12}c_{21} = \frac{1}{R_1} \cdot \frac{1}{R_2} \equiv K, \quad (3.51)$$

which we call the *Gaussian curvature*.

Computing the trace and determinant of a given  $2 \times 2$  is not so difficult. With a little more work, we can find the eigenvalues; the inverse eigenvalues  $R_1$  and  $R_2$  are called the *principal radii of curvature*.

How can we write an *energy* which is invariant under coördinate transformations? Recall the Hooke law for elasticity in a spring: the elastic energy is quadratic in displacement. The Gaussian curvature  $K$  is already quadratic;  $H$  is linear, so we would include an  $H^2$  term, although we might wish to subtract a constant corresponding to the rest length of a spring. Including a constant term to incorporate surface tension effects, we can write the energy functional

$$E = \int dA \left[ \gamma + \frac{\kappa}{2} (H - H_0)^2 + \bar{\kappa} K \right]. \quad (3.52)$$

In Eq. (3.52),  $\gamma$  parameterizes the surface tension,  $\kappa$  is the “bending rigidity”, and  $H_0$  is the “spontaneous curvature”. (Such a spontaneous curvature requires an asymmetry between the two sides of the membrane, and could be an effect of two different kinds of molecules in a bilayer.) The parameter  $\bar{\kappa}$  is called the “Gaussian rigidity”.

The theory of Eq. (3.52) is good for a soap bubble but not so good for a piece of paper, and it is even worse for a rubber balloon. Why? The soap film is essentially *fluid*: there is no energy associated with shear stresses. Such is not the case with a rubber sheet, although since shearing paper is more difficult, Eq. (3.52) is not so bad a representation.

We do not always need all the parameters of Eq. (3.52) to describe the situation. For example, the *Gauss-Bonnet theorem* tells us that for all shapes topologically equivalent to a sphere,

$$\int dA K = 4\pi.$$

Deformations of the sphere do not change the integral; they all manage to cancel out. This result is actually more general. For a surface with Euler characteristic  $\chi_E$ ,

$$\boxed{\int dA K = 4\pi\chi_E.} \quad (3.53)$$

Furthermore, in many cases involving lipid bilayers,  $\gamma \approx 0$ . The reason is that the phospholipid layers are typically immersed in a solution containing phospholipid molecules, allowing exchanges to take place. (The exact mechanism here doesn't matter too much; the fact that  $\gamma \approx 0$  can be taken as an experimental result.)

For small deformations around a flat surface, we use the ‘‘Monge’’ representation. Over a reasonably-sized patch, we can describe the surface by a function  $h(x_1, x_2)$ . The energy is then given by

$$E = \int dx_1 dx_2 \sqrt{1 + \left(\frac{\partial h}{\partial x_1}\right)^2 + \left(\frac{\partial h}{\partial x_2}\right)^2} \left[ \gamma + \frac{\kappa}{2} (\nabla^2 h)^2 \right]. \quad (3.54)$$

Neglecting things I'll justify when I have Kardar's notes,

$$E = \frac{\kappa}{2} \int dx_1 dx_2 (\nabla^2 h)^2. \quad (3.55)$$

How does the Laplacian operator act upon the curvature?

$$\begin{aligned} \nabla^2 \left( \frac{1}{2} \sum_{i,j} c_{ij} x_i x_j \right) &= c_{11} + c_{22} \\ &= 2H. \end{aligned}$$

This image of undulations is easily transferred into the language of Fourier transforms.

$$h(\vec{x}) = \sum_{\vec{q}} e^{i\vec{q}\cdot\vec{x}} \tilde{h}_{\vec{q}}. \quad (3.56)$$

The Laplacian becomes

$$\nabla^2 h = \sum_{\vec{q}} (-q^2) e^{i\vec{q}\cdot\vec{x}} \tilde{h}_{\vec{q}}, \quad (3.57)$$

giving an energy

$$E = \sum_{\vec{q}} \frac{\kappa}{2} q^4 |\tilde{h}_{\vec{q}}|^2. \quad (3.58)$$

By equipartition, the expectation value for the  $q$ -th mode is

$$\langle |\tilde{h}_{\vec{q}}|^2 \rangle = \frac{k_B T}{\kappa q^4}. \quad (3.59)$$

## 4 27 April 2005

We ended the last lecture talking about the fluctuations of a membrane. As we demonstrated, the energy due to bending can be written in terms of Fourier modes  $q = 2\pi/\lambda$ . Eq. (3.59) indicates that the amplitudes of each oscillation mode increase for longer and longer wavelengths, thanks to the  $1/q^4$  dependence.

In terms of the net fluctuations,

$$\begin{aligned} w^2 &= \sum_q \langle |\tilde{h}_q|^2 \rangle \\ &= \frac{k_B T}{\kappa} \int \frac{d^3 \vec{q}}{(2\pi)^2} \frac{1}{q^4} \\ &= \frac{k_B T}{2\pi\kappa} \int_{\pi/L}^{\pi/a} \frac{dq}{q^3}, \end{aligned}$$

where the upper and lower limits of the integral are only approximate.  $L$  is the linear size of the membrane patch, and  $a$  denotes its thickness.

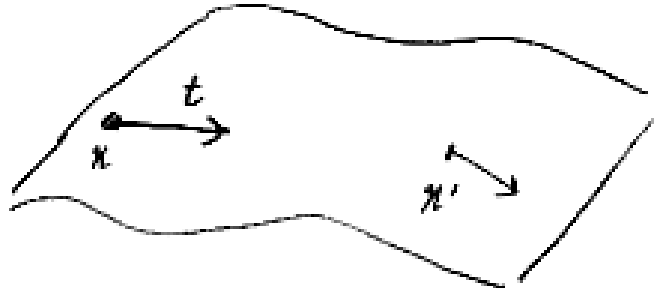
$$w^2 = \frac{k_B T}{4\pi\kappa} \cdot \frac{L^2}{\pi^2}. \quad (4.1)$$

Since  $w^2 \propto L^2$ , the ratio of interest is  $w/L$ , or

$$\frac{w}{L} = \sqrt{\frac{1}{4\pi^3 \left(\frac{\kappa}{k_B T}\right)}}. \quad (4.2)$$

For typical membranes, the ratio  $\kappa/k_B T \approx 2$  to 20. Consequently,  $w/L \approx 1/20$ , so for a patch of size  $L = 2 \mu\text{m}$ , the oscillations will be of size  $w \approx 0.1 \mu\text{m}$ .

Motivated by our earlier work with polymers, we can ask if these membranes exhibit a *persistence length*. For instance, if we fix one edge of the membrane patch to be horizontal, how far do we have to move before the membrane orientation is uncorrelated?



It turns out that the persistence length is also governed by the ratio  $\kappa/k_B T$ :

$$l_P \approx a \exp\left(\frac{c\kappa}{k_B T}\right). \quad (4.3)$$

#### 4.0.1 Red Blood Cells

Suppose we have a cell whose membrane is described by Eq. (3.52). What shape minimizes this cell's surface-related energy? The answer is obvious: a sphere whose radius is the preferred radius  $1/H_0$ . One way to alter this situation is to add extra constraints, say a requirement that the *volume* of the cell be fixed.

“The elasticity of these cells is complicated, but not *too* complicated. It is within the realm of things we can think about using standard tools of elasticity.”

#### 4.0.2 Transport Across Membranes

Hydrophobic molecules such as  $O_2$ ,  $CO_2$ ,  $N_2$  and benzene can pass through a lipid bilayer, but smaller ions such as  $H^+$ ,  $Na^+$  and  $K^+$  cannot. This is due to an *electrostatic barrier*. In water, an ion “feels” a dielectric constant around 80, but within the lipid bilayer, the dielectric constant is of order 1. This creates an energy barrier of almost two orders of magnitude, making it unfavorable for ions to enter (and thereby pass through) the cell membrane. In cases where it is biologically necessary for ions to be transported across the membrane, Nature must provide special opportunities to do so.

One such device is a passive ion channel, essentially a tube of protein placed in the bilayer, giving a place for ions to pass through. These devices cannot be the whole story, however, since the concentrations of many common ions are radically out of balance between the inside and the outside of the cell. What we require is a Maxwell's Demon, a mechanism which consumes energy to actively maintain a concentration gradient.

The concentration differences of these charged ions lead to membrane potentials, described by the *Nernst equation*:

$$\phi = \frac{k_B T}{ez} \log\left(\frac{n_1}{n_2}\right) \quad (4.4)$$

The order of magnitude is set by  $k_B T/e$ , which is around 25 mV.

Next, we take up the topic of cell motion. The classic paper is Ed Purcell's “Life at Low Reynolds Number”, *Am. J. Phys.* **45**(1), 1977.